Magnetic properties and neutron diffraction study of double perovskites Ca_2LnRuO_6 (Ln = Y, La–Lu)

2005 J. Phys.: Condens. Matter 17 7383

(http://iopscience.iop.org/0953-8984/17/46/022)

INSTITUTE OF PHYSICS PUBLISHING JOURNAL OF PHYSICS: CONDENSED MATTER

J. Phys.: Condens. Matter **17** (2005) 7383–7394 doi:10.1088/0953-8984/17/46/022

Magnetic properties and neutron diffraction study of double perovskites Ca_2LnRuO_6 (Ln = Y, La–Lu)

Chiho Sakai[1], **Yoshihiro Doi**[1], **Yukio Hinatsu**[1] **and Kenji Ohoyama**[2]

[1] Division of Chemistry, Graduate School of Science, Hokkaido University, Sapporo 060-0810, Japan
[2] Institute for Materials Research, Tohoku University, Sendai 980-8577, Japan

Received 12 August 2005, in final form 30 September 2005
Published 1 November 2005
Online at stacks.iop.org/JPhysCM/17/7383

Abstract

Magnetic properties of double perovskites Ca_2LnRuO_6 (Ln = Y, La–Lu) were investigated. From the magnetic susceptibility and specific heat measurements, it is found that all the title compounds show an antiferromagnetic transition (T_N = 10–34 K), and that the antiferromagnetic ordering of Ru^{5+} ions with a doublet ground state occurs below these temperatures. In these compounds, the larger Ln ions tend to occupy the A site of the perovskite ABO_3, while the smaller Ln ions tend to occupy the B site. The Nd ions in Ca_2NdRuO_6 are situated at the A site and show an antiferromagnetic transition at 1.6 K, which is much lower than T_N = 11.5 K. On the other hand, the Yb ions in Ca_2YbRuO_6 are situated at the B site, and a long-range antiferromagnetic ordering due to both Yb^{3+} and Ru^{5+} ions occurs at 34 K. The magnetic structure of Ca_2YbRuO_6 was determined by powder neutron diffraction measurements; it shows a non-collinear arrangement between Yb^{3+} ($\sim$1.3 μ_B) and Ru^{5+} ($\sim$1.7 μ_B) moments.

1. Introduction

In recent years, the solid-state chemistry of mixed metal oxides containing platinum group metals has attracted a great deal of interest. In such oxides, the perovskite-related compounds containing ruthenium show a wide range of electronic properties [1, 2]. The crystal structure of the perovskite oxide ABO_3 can be described as a framework of corner-shared BO_6 octahedra, which contains A cations at 12-coordinate sites. Since the B cations generally determine the physical properties of perovskites, the combination of different kinds of B cations (B′ and B″ cations), ruthenium and other metals, may bring about attractive and unusual properties.

When the size and/or charge of the B′ and B″ cations are sufficiently different, $AB'_{0.5}B''_{0.5}O_3$ can order, doubling the formula unit. The structural chemistry and magnetic properties of the double perovskites A_2LnRuO_6 (A = Sr, Ba; Ln = Y, lanthanide elements) have been investigated [3–18]. In them, the Ln and Ru ions are regularly ordered, i.e., the rock-salt type arrangement is observed over the six-coordinate B sites. These compounds show an antiferromagnetic transition at 26–117 K. When the Ln ion is magnetic, a complicated

temperature dependence of the magnetic susceptibilities is observed below the transition temperatures, reflecting the magnetic interaction between Ru and Ln ions.

Now, our attention has been focused on double perovskite oxides having Ca ions at the A site, Ca_2LnRuO_6. Different from the case for the analogous Sr and Ba compounds, Ca_2LnRuO_6 show a partial structural disordered arrangement between the Ca and Ln sites [5, 9, 19]. Therefore, these compounds should be represented by $Ca_{2-x}Ln_x[Ln_{1-x}Ca_x]RuO_6$ [9, 19]. Our recent studies on their crystal structures reveal that the ratio of the Ln substitution for Ca, x, varies with the ionic radius of the Ln ion: the larger Ln ions occupy the A site, while the smaller Ln ions tend to occupy the B site [19]. Magnetic properties of Ca_2LnRuO_6 have been reported for Ln = Y [7], La [5], Nd [9], Eu [3, 4], Ho [9], and Lu [19] (most of these Ln ions are non-magnetic). However, the crystal structure and magnetic properties of Ca_2LnRuO_6 compounds including magnetic Ln ions have not been studied in detail yet. Studying such compounds should give some information about the magnetic interaction between d (Ru) and f (Ln) electrons.

In this work, we have investigated the magnetic properties of a series of Ca_2LnRuO_6 compounds (Ln = Y, La–Lu) through magnetic susceptibility and specific heat measurements. For Ca_2YbRuO_6, powder neutron diffraction experiments were carried out to determine its magnetic structure.

2. Experimental details

Polycrystalline samples of Ca_2LnRuO_6 were prepared by a solid-state reaction as described elsewhere [19]. Magnetic susceptibility measurements were performed under both the zero-field-cooled (ZFC) and field-cooled (FC) conditions with a SQUID magnetometer (Quantum Design MPMS model) in the temperature range of 1.8–300 K. The applied magnetic field was 0.1 T. The specific heat was measured for Ln = Y, La, Nd, and Yb compounds by a relaxation technique using a physical property measurement system (Quantum Design, Model PPMS) in the temperature range of 1.8–300 K. The sample in the form of a pellet (∼10 mg) was mounted on an alumina plate with Apiezon grease for better thermal contact.

The powder neutron diffraction profiles for Ca_2YbRuO_6 were measured using the Kinken Powder Diffractometer for High Efficiency and High Resolution Measurement, HERMES, of the Institute for Materials Research (IMR), Tohoku University [20], installed at the JRR-3M Reactor in the Japan Atomic Energy Research Institute (JAERI), Tokai. The measurements were carried out at 2.3 and 50 K in the range $3^\circ \leqslant 2\theta \leqslant 153^\circ$ at intervals of 0.1° with the wavelength of 1.820 35 Å. The neutron diffraction data were analysed by the Rietveld technique, using the program FullProf [21]. The magnetic form factor for the Ru^{5+} ion in [22] was used. A small amount (∼2%) of an impurity phase Yb_2O_3 was detected in the Ca_2YbRuO_6; its diffraction peaks were also fitted as a second phase.

3. Results and discussion

3.1. Magnetic properties for Ca_2LnRuO_6 (Ln = Y, La, Lu)

The reciprocal magnetic susceptibilities of Ca_2LnRuO_6 (Ln = Y, La, Lu) are plotted as a function of temperature in figure 1. Magnetic properties of Ca_2LnRuO_6 (Ln = Y, La, Lu) are due to the Ru^{5+} ion because these Ln^{3+} ions are diamagnetic. Table 1 lists the effective magnetic moments and Weiss constants determined by the Curie–Weiss law fitting. The effective magnetic moments are close to the spin-only value for the Ru^{5+} ion with $S = 3/2$. The large negative Weiss constants indicate the antiferromagnetic interaction between Ru^{5+} ions.

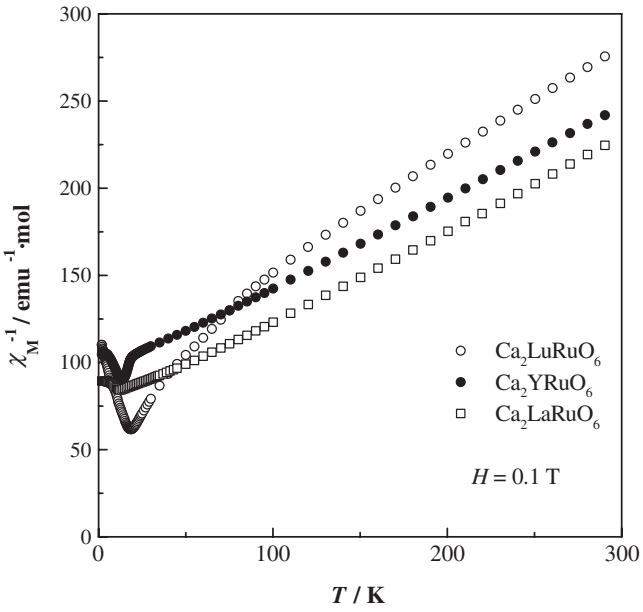

Figure 1. Temperature dependence of the reciprocal magnetic susceptibilities for Ca_2LnRuO_6 (Ln = Y, La, Lu).

Table 1. Magnetic parameters for Ca_2LnRuO_6.

Ln	μ_{eff}(cal) (μ_B)	μ_{eff}(exp) (μ_B)	θ (K)
Y	3.87	3.74(1)	−155(1)
La	3.87	3.72(1)	−115(2)
Pr	5.27	5.17(1)	−75.2(8)
Nd	5.30	5.19(1)	−69.3(3)
Sm	4.17	3.59[a]	—
Eu	5.15	4.70[a]	—
Gd	8.83	8.63(1)	−1.5(2)
Tb	10.46	10.36(1)	−12.1(3)
Dy	11.31	11.14(1)	−15.5(5)
Ho	11.27	11.14(2)	−17.3(8)
Er	10.34	10.03(6)	−17(3)
Tm	8.48	8.30(2)	−47(1)
Yb	5.97	5.33(9)	−105(6)
Lu	3.87	3.67(9)	−162(13)

[a] Observed values at room temperature.

These compounds show an antiferromagnetic transition at low temperatures. Their Néel temperatures (T_N) are listed in table 2, and those for the analogous Sr and Ba compounds are also listed. A clear tendency is found for the T_N of A_2LnRuO_6 with the same Ln ions, i.e., $T_N(A = Ba) > T_N(Sr) > T_N(Ca)$. This is due to the change in the tilting between LnO_6 and RuO_6 octahedra in A_2LnRuO_6. When the size of the A cation is not so much larger than that of the B cation, the tilting between BO_6 octahedra often occurs. The tilting angles (∠Ru–O–Ln) in A_2LnRuO_6 are ∼180° for A = Ba, ∼158° for Sr, and ∼145° for Ca; the structure of the Ca compounds is highly distorted, which is illustrated in figure 2. The structural distortion should

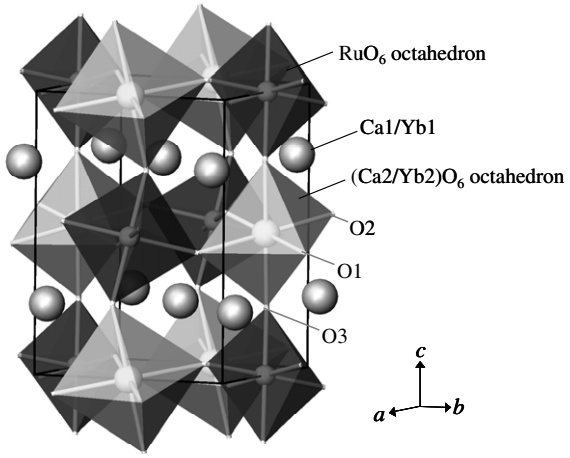

Figure 2. Crystal structure for Ca_2YbRuO_6 determined by the neutron diffraction measurements at 50 K.

Table 2. The Néel temperatures for double perovskites A_2LnRuO_6.

	A					
Ln	Ba	[Ref]	Sr	[Ref]	Ca	[Ref]
Y	37	[15]	26	[6]	14	This work
La	29.5	[5]	—		11.5	This work
Pr	117	[14]	—		10	This work
Nd	57	[13]	—		11.5	This work
Sm	54	[23]	—		10	This work
Eu	42	[4]	31	[4]	18	[4]
Gd	48	[23]	36	[10]	10	This work
Tb	58	[23]	41	[12]	11	This work
Dy	47	[23]	44	[10]	11	This work
Ho	51	[17]	36	[11]	12	This work
Er	40	[15]	42	[10]	16	This work
Tm	42	[16]	36	[16]	17	This work
Yb	48	[16]	44	[16]	34	This work
Lu	35	[8]	30	[8]	14	This work

weaken the superexchange magnetic interaction between Ru ions via the Ru–O–Ln–O–Ru or Ru–O–O–Ru pathway and then decrease the magnetic transition temperature.

In the case of Ca_2LnRuO_6 compounds, a partial structural disordered arrangement is found between Ca and Ln sites, and they should be described as $Ca_{2-x}Ln_x[Ln_{1-x}Ca_x]RuO_6$ [19]. For Ln = Y, La, Lu compounds, the substitution parameters x are $x = 1$ for Ln = La, $x = 0.442$ for Y, and $x = 0.071$ for Lu. However, the T_N values for Ca_2LnRuO_6 (Ln = Y, La, Lu) are comparable, which means that the influence of Ca and Ln disordered arrangement on the T_N is not observed. The reason for this is that these lanthanide ions (Ln = Y, La, Lu) are diamagnetic.

Figure 3(a) shows the temperature dependence of the specific heat for Ca_2LaRuO_6. A λ-type anomaly is found at 11.5 K, which agrees with T_N observed in the magnetic susceptibility. Then, we evaluated the magnetic entropy change due to the magnetic ordering of Ru^{5+} ions

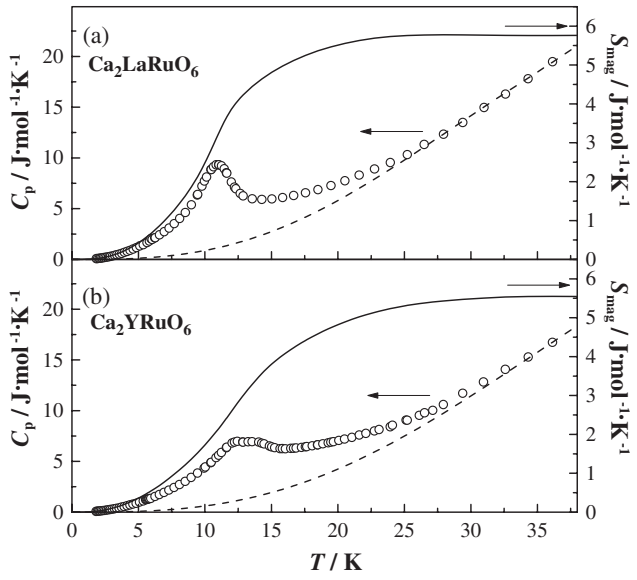

Figure 3. Temperature dependences of the specific heat and magnetic entropy for (a) Ca_2LaRuO_6 and (b) Ca_2YRuO_6. Dashed lines are the lattice and electronic specific heats estimated by calculation (see the text).

from the specific heat data. To calculate the magnetic specific heat (C_{mag}), the lattice and electronic contributions must be subtracted from the total specific heat. They were estimated by using a polynomial function of the temperature, $f(T) = aT^3 + bT^5 + cT^7$ [24], in which the coefficients were determined by fitting this function to the observed specific heat data between 30 and 45 K. From the temperature dependence of the magnetic specific heat, the magnetic entropy change of Ca_2LaRuO_6 is calculated by the relation $S_{mag} = \int (C_{mag}/T)\,dT$ and its temperature dependence is also shown in figure 3(a). The magnetic entropy change (ΔS_{mag}) due to the antiferromagnetic ordering of Ru^{5+} ions is about 5.8 J mol^{-1} K^{-1}.

In a similar way as for Ca_2LaRuO_6, the temperature dependences of the specific heat and magnetic entropy for Ca_2YRuO_6 are shown in figure 3(b). A broad specific heat anomaly is observed around 13 K, which corresponds to the result for magnetic susceptibility measurements. The ΔS_{mag} derived from this anomaly is determined to be 5.5 J mol^{-1} K^{-1}. Recently, we have performed the specific heat measurements for Ca_2LuRuO_6 and obtained approximately the same value for ΔS_{mag} (5.3 J mol^{-1} K^{-1}). The ΔS_{mag} values for these three compounds are very close to $R \ln 2 = 5.76$ J mol^{-1} K^{-1} rather than the $R \ln 4 = 11.53$ J mol^{-1} K^{-1} expected from the $S = 3/2$ ground state (R: molar gas constant). This fact means that the fourfold-degenerate ground state of the Ru^{5+} ion splits into two Kramers' doublet states.

3.2. Magnetic susceptibility for Ca_2LnRuO_6 (Ln = Pr, Nd, Sm–Yb)

The temperature dependence of reciprocal magnetic susceptibilities for Ca_2LnRuO_6 (Ln = magnetic ions) is shown in figure 4. The effective magnetic moments and Weiss constants are listed in table 1. The experimental effective magnetic moments μ_{eff}(exp) are in good agreement with the calculated ones from the equation μ_{eff} (cal) $= \sqrt{\mu^2_{Ru^{5+}} + \mu^2_{Ln^{3+}}}$. The negative Weiss constants indicate that the predominant interaction is antiferromagnetic. The

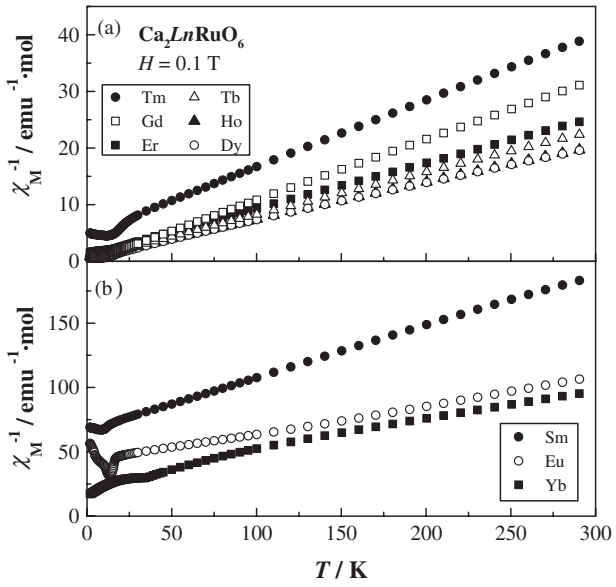

Figure 4. Temperature dependence of the reciprocal magnetic susceptibilities of Ca_2LnRuO_6 (Ln = Pr, Nd, Sm–Yb).

magnetic susceptibilities of Ca_2SmRuO_6 and Ca_2EuRuO_6 do not obey the Curie–Weiss law because of the influence of excited states of Ln^{3+} ions: ^6H_J ($J = 7/2, 9/2, \ldots, 15/2$) for the Sm^{3+} ion and ^7F_J ($J = 1, 2, \ldots, 6$) for the Eu^{3+} ion. Thus, $\mu_{\rm eff}$(exp) is the moment observed at 300 K and the values for $\mu_{\rm eff}$(cal) are calculated by the Van Vleck equation [25].

At low temperatures, all the compounds show antiferromagnetic transitions, and the Néel temperatures are summarized in table 2. The same tendency for T_N as that observed in Ln = Y, La, Lu compounds is observed. That is, for the A_2LnRuO_6 compounds with the same Ln ions, T_N is in the order T_N(A = Ba) > T_N(Sr) > T_N(Ca). Additionally, it is found that the T_N for Ca_2YbRuO_6 is much higher than those for the other Ca_2LnRuO_6 compounds. This result can be connected with the degree of the structural disordered arrangement between Ca and Ln ions. The substitution parameters x in $Ca_{2-x}Ln_x[Ln_{1-x}Ca_x]RuO_6$ are 1 (for Ln = Pr), 0.980 (Nd), 0.975 (Sm), 0.942 (Eu), 0.933 (Gd), 0.929 (Tb), 0.840 (Dy), 0.539 (Ho), 0.237 (Er), 0.106 (Tm) and 0.096 (Yb) [19]; the larger Ln ions (Ln = Pr, Nd, Sm–Ho) mainly occupy the A site, while the smaller ones (Ln = Er–Yb) occupy the B site. In the former case, the substitution of non-magnetic Ca^{2+} ion for Ln^{3+} ion at the B site should weaken the magnetic interaction of Ca_2LnRuO_6 compounds. In the latter case, the magnetic interaction between Ln and Ru ions via the Ln–O–Ru pathway should contribute to the antiferromagnetic transition. Compared with the T_N for Ca_2YbRuO_6, the T_N for the Er and Tm compounds may be lowered by the magnetic dilution with non-magnetic Ca^{2+} ions and furthermore the Tm^{3+} ion is the non-Kramers ion. In the next section, we report the detailed magnetic properties for Ca_2NdRuO_6 ($x = 0.980$) and Ca_2YbRuO_6 ($x = 0.096$).

3.3. Magnetic properties of Ca_2NdRuO_6

The molar magnetic susceptibility of Ca_2NdRuO_6 is plotted as a function of temperature in figure 5(a). This compound shows the antiferromagnetic transition at 11.5 K. In the case of Ca_2NdRuO_6, almost all Nd^{3+} ions occupy the A site ($x = 0.980$). According to the

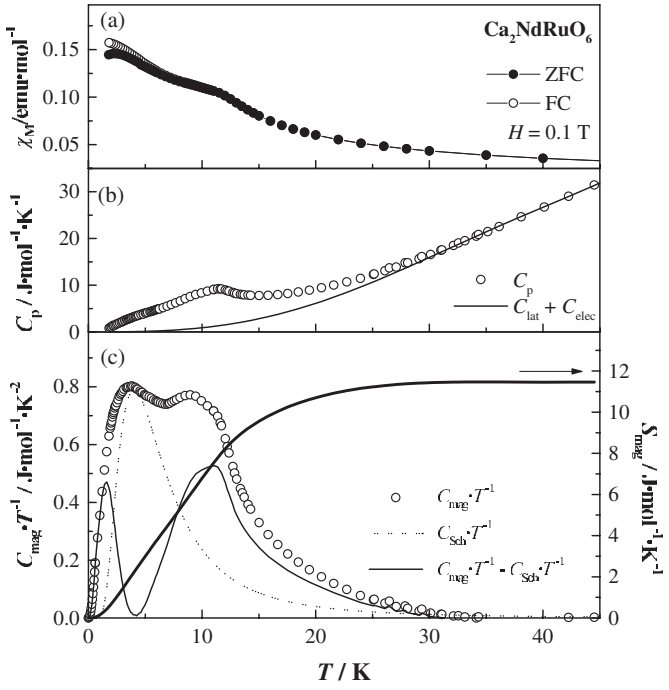

Figure 5. Temperature dependences of (a) the magnetic susceptibility, (b) specific heat, and (c) magnetic specific heat and magnetic entropy for Ca_2NdRuO_6.

previous neutron diffraction measurements at 4.2 K [9], the magnetic moments of the Ru^{5+} ions order antiferromagnetically (type I), but there is no evidence for the magnetic ordering of Nd^{3+} moments. In addition, this transition temperature is almost the same as that of the La compound. These facts indicates that the magnetic interaction between Nd^{3+} and Ru^{5+} ions hardly contribute to this antiferromagnetic transition. At still lower temperatures (∼2.1 K), another small anomaly is observed, and this anomaly may be a magnetic ordering of Nd^{3+} at the A site. In order to clarify detailed magnetic properties of this compound, specific heat measurements were carried out.

The temperature dependence of the specific heat for Ca_2NdRuO_6 is shown in figure 5(b). The magnetic specific heat (C_{mag}) and magnetic entropy (S_{mag}) are calculated from the specific heat data in the same way as is the case for Ca_2LaRuO_6. The C_{mag}/T and S_{mag} curves are plotted in figure 5(c). It is found that the C_{mag}/T curve shows two anomalies at 11.5 and 4.5 K. The total magnetic entropy change due to these two anomalies is approximately 11.4 J mol^{-1} K^{-1}, which is close to the value of $2R \ln 2 = 11.53$ J mol^{-1} K^{-1}. The anomaly at 11.5 K corresponds to the antiferromagnetic transition observed in the magnetic susceptibility. In comparison with the La compound, ΔS_{mag} due to the magnetic ordering of Ru^{5+} ions is expected to be $R \ln 2 = 5.76$ J mol^{-1} K^{-1}. Thus, the rest of ΔS_{mag} ($\sim R \ln 2$) should be the contribution from the Nd^{3+} ion. This result also indicates that the ground state of Nd^{3+} ion should be a Kramers' doublet.

For the specific heat anomaly at 4.5 K, the corresponding anomaly is not observed in the magnetic susceptibility measurements. No long-range magnetic ordering of Nd^{3+} ions has been observed in the previous neutron diffraction measurements down to 4.2 K [9]. Namely, the Nd^{3+} ion is still in the paramagnetic state at around 4.5 K. We considered that the observed

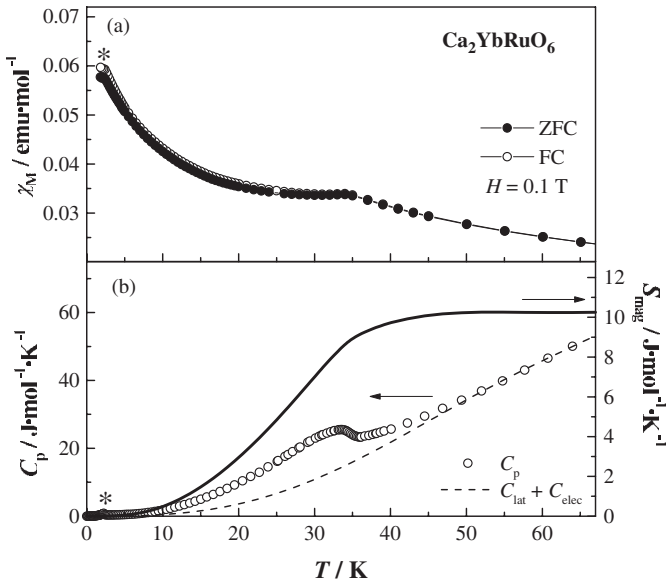

Figure 6. Temperature dependence of (a) the magnetic susceptibility, (b) specific heat and magnetic entropy for Ca_2YbRuO_6. The asterisk shows the antiferromagnetic transition of impurity phase Yb_2O_3.

anomaly is due to not the magnetic ordering, but the Schottky-type anomaly of the Nd^{3+} ion. The ground multiplet $^4I_{9/2}$ of Nd^{3+} splits into five Kramers' doublets in a low symmetry crystal field; the observed magnetic entropy of $R \ln 2$ indicates that the ground doublet is selectively populated at low temperatures. Additionally, this doublet should be split by the internal magnetic field produced by the antiferromagnetic ordering of Ru^{5+} ions. The Schottky specific heat (C_{Sch}) by thermal population between two level states is represented by

$$C_{Sch} = \frac{R(\Delta/k_BT)^2(g_0/g_1)\exp(\Delta/k_BT)}{[1+(g_0/g_1)\exp(\Delta/k_BT)]^2} \tag{1}$$

where Δ is the energy difference by the Zeeman splitting, k_B is the Boltzmann constant, and g_0 and g_1 are the multiplets of ground and excited states (in the present case $g_0 = g_1 = 1$). The Schottky specific heat calculated by using $\Delta \sim 13$ K is added as a dotted line in figure 5(c), which shows a good fit to the observed anomaly. We subtracted this Schottky specific heat (C_{Sch}) from the magnetic specific heat (C_{mag}), and the resultant specific heat is also plotted against temperature in figure 5(c). It shows a peak at 1.6 K. This may be due to an antiferromagnetic ordering of Nd^{3+} ions.

3.4. Magnetic properties of Ca_2YbRuO_6

The magnetic susceptibility, specific heat, and magnetic entropy for Ca_2YbRuO_6 at low temperatures are plotted in figure 6. The specific heat shows a λ-type anomaly at 34 K, which corresponds to the result of the magnetic susceptibility. In addition, another anomaly is observed at 2.3 K in both graphs. This is due to an antiferromagnetic transition of an impurity Yb_2O_3 [26]. The contribution derived from this impurity was excluded from S_{mag}. The ΔS_{mag} for the magnetic transition observed at 34 K is determined to be 10.2 J mol^{-1} K^{-1}. This value is comparable to $2R \ln 2 = 11.53$ J mol^{-1} K^{-1}; thus, it is concluded that both Yb^{3+} and Ru^{5+} ions in the doublet ground state order antiferromagnetically in the Ca_2YbRuO_6 compound.

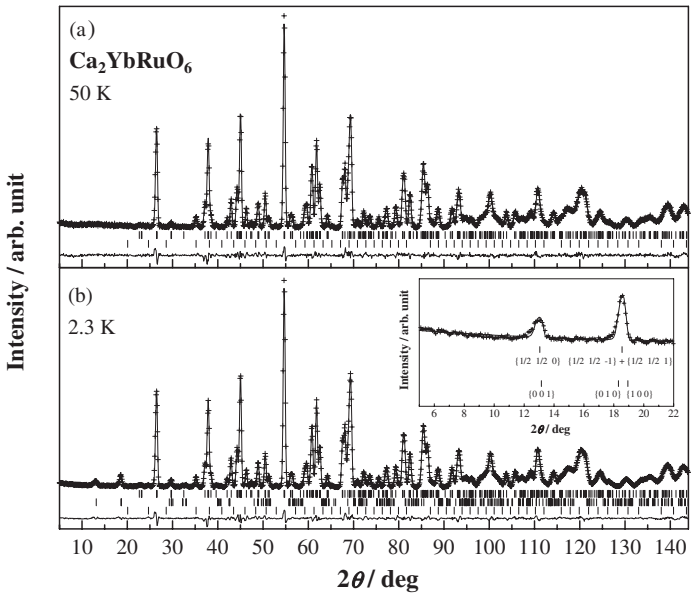

Figure 7. Powder neutron diffraction profiles for Ca_2YbRuO_6 at (a) 50 K and (b) 2.3 K. The upper and middle vertical marks represent the nuclear and magnetic reflections for Ca_2YbRuO_6, and bottom marks represent the nuclear reflections for the impurity Yb_2O_3 phase. The inset graph of (b) shows calculated peak positions using different models for the magnetic structure (see text).

Table 3. Structural parameters for Ca_2YbRuO_6 determined by the neutron diffraction measurements at 50 K. (Note: space group $P2_1/n$; $a = 5.5153(1)$ Å, $b = 5.7011(1)$ Å, $c = 7.9059(2)$ Å, $\beta = 90.314(2)°$, $R_{wp} = 8.95\%$, $R_p = 7.70\%$, $R_e = 6.38\%$.)

Atom	Site	Occupancy	x	y	z	B (Å^2)
Ca1	4e	0.952(3)	0.5156(8)	0.5561(4)	0.2500(8)	0.42(8)
Yb1	4e	0.048	0.5156	0.5561	0.2500	0.42
Ca2	2c	0.096	0	1/2	0	0.01(3)
Yb2	2c	0.904	0	1/2	0	0.01
Ru	2d	1.0	1/2	0	0	0.01
O1	4e	1.0	0.2138(6)	0.1866(6)	−0.0520(5)	0.26(4)
O2	4e	1.0	0.3179(7)	0.7175(7)	−0.0580(5)	0.26
O3	4e	1.0	0.3957(5)	−0.0404(5)	0.2341(5)	0.26

Figure 7 shows the powder neutron diffraction profiles at 50 and 2.3 K. The data at 50 K are well fitted with the same structural model as we used in the analysis of previous x-ray diffraction data [19]; no structural change is observed except for the contraction of the unit cell at low temperatures. The determined structural parameters, and bond lengths and bond angles, are listed in tables 3 and 4, respectively.

In the profile measured at 2.3 K, some additional reflection peaks were found at lower angles, which were not observed at 50 K. They are associated with the long-range ordering of magnetic moments for Yb^{3+} and Ru^{5+}. The enlarged profile at lower angles is shown in the inset graph of figure 7(b). The peak positions of magnetic reflections are near to {0 0 1}, {1 0 0}, {0 1 0}, ..., which have been observed in many A_2LnRuO_6 compounds with a monoclinic structure [16]. However, the analysis using the same magnetic structural model

Table 4. Bond lengths and bond angles for Ca_2YbRuO_6 determined by the neutron diffraction at 50 K.

Bond lengths (Å)			
Yb2/Ca2–O1	2.181(4) × 2	Ru–O1	1.945(3) × 2
Yb2/Ca2–O2	2.198(4) × 2	Ru–O2	1.952(4) × 2
Yb2/Ca2–O3	2.189(4) × 2	Ru–O3	1.955(4) × 2
Bond angles (deg)			
O1–Yb2/Ca2–O2	90.6(2)	O1–Ru–O2	90.8(2)
O1–Yb2/Ca2–O3	92.6(1)	O1–Ru–O3	91.3(1)
O2–Yb2/Ca2–O3	93.1(1)	O2–Ru–O3	91.6(1)
Yb2/Ca2–O1–Ru	147.9(2)	Yb2/Ca2–O1–Ru	147.9(2)
Yb2/Ca2–O2–Ru	145.8(2)	Yb2/Ca2–O2–Ru	145.8(2)
Yb2/Ca2–O3–Ru	145.1(1)	Yb2/Ca2–O3–Ru	145.1(1)

Table 5. Structural parameters for Ca_2YbRuO_6 determined by the neutron diffraction measurements at 2.3 K. (Note: space group $P2_1/n$; $a = 5.5149(1)$ Å, $b = 5.7005(1)$ Å, $c = 7.9058(2)$ Å, $\beta = 90.307(2)^\circ$, $R_{wp} = 6.81\%$, $R_p = 5.69\%$, $R_e = 2.84\%$, $R_{mag} = 6.95\%$, $\boldsymbol{k} = (1/2, 1/2, 0)$, $\mu_{Yb2} = 1.3(3)\ \mu_B$ ($\mu \parallel a$, $0.3(3)\ \mu_B$; $\mu \parallel b$, $-0.6(3)\ \mu_B$; $\mu \parallel c$, $1.1(2)\ \mu_B$), $\mu_{Ru} = 1.7(4)\ \mu_B$ ($\mu \parallel a$, $-1.1(5)\ \mu_B$; $\mu \parallel b$, $1.2(4)\ \mu_B$; $\mu \parallel c$, $0.4(4)\ \mu_B$).)

Atom	Site	Occupancy	x	y	z	B (Å^2)
Ca1	4e	0.952	0.5164(6)	0.5564(3)	0.2498(7)	0.39(4)
Yb1	4e	0.048	0.5164	0.5564	0.2498	0.39
Ca2	2c	0.096	0	1/2	0	0.03(3)
Yb2	2c	0.904	0	1/2	0	0.03
Ru	2d	1.0	1/2	0	0	0.03
O1	4e	1.0	0.2138(5)	0.1869(5)	−0.0517(4)	0.24(3)
O2	4e	1.0	0.3182(5)	0.7167(5)	−0.0582(4)	0.24
O3	4e	1.0	0.3952(4)	−0.0404(4)	0.2336(4)	0.24

as that used for A_2LnRuO_6 compounds ended in failure. Finally, it is found that all the observed reflection positions can be indexed using a propagation vector $\boldsymbol{k} = (1/2\ 1/2\ 0)$. In order to determine the magnetic structure, we assumed that each of the Yb^{3+} and Ru^{5+} moments orders antiferromagnetically and that the ferromagnetic component was ignored since the ferromagnetic moment expected from the difference between ZFC and FC magnetic susceptibilities was at most $\sim 10^{-4}\ \mu_B$. The structural parameters determined by the Rietveld analysis are listed in table 5, and the magnetic structure is represented in figure 8. In this magnetic structure, the ordered magnetic moments of Yb^{3+} and Ru^{5+} ions adopt a non-collinear arrangement at angles of $\sim 106^\circ$ (or 74°). Their magnitudes are determined to be $1.3(3)\ \mu_B$ and $1.7(4)\ \mu_B$, respectively; both values are reasonable as compared with the previous results of the neutron diffraction measurements for A_2LnRuO_6 [16].

4. Summary

Magnetic properties of the double perovskites Ca_2LnRuO_6 (Ln = Y, La–Lu) were investigated. These compounds should be represented as $Ca_{2-x}Ln_x[Ln_{1-x}Ca_x]RuO_6$; the larger Ln ions occupy the A site, while the smaller Ln ions tend to occupy the B site. These compounds show an antiferromagnetic transition at 10–34 K, and the antiferromagnetic ordering of Ru^{5+} ions occurs below these temperatures. The Nd ions in Ca_2NdRuO_6 show an antiferromagnetic

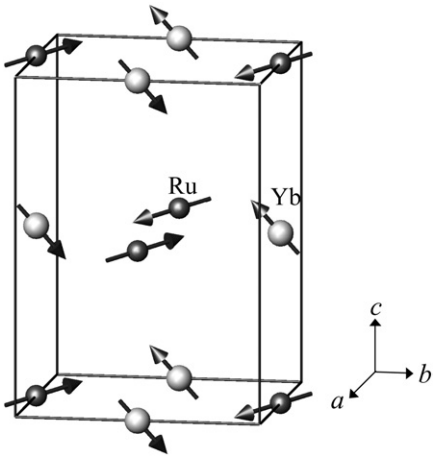

Figure 8. One-quarter of the magnetic structure for Ca_2YbRuO_6. The direction of the magnetic moments for both Yb^{3+} and Ru^{5+} ions changes complying with the propagation vector $\boldsymbol{k} = (1/2, 1/2, 0)$.

transition at 1.6 K, which is much lower than $T_N = 11.5$ K. In Ca_2YbRuO_6, both the Yb^{3+} and Ru^{5+} ions show a long-range antiferromagnetic ordering at 34 K. This transition temperature is much higher than those for the other compounds ($T_N = 10$–18 K). These results indicate that when Ln ions occupy the B site in the double perovskite, the magnetic interaction between 4d and 4f electrons becomes stronger and both the magnetic moments contribute to its antiferromagnetic transition. The magnetic structure of Ca_2YbRuO_6 was determined by powder neutron diffraction measurements; it shows a non-collinear arrangement between Yb^{3+} ($\sim$1.3 μ_B) and Ru^{5+} ($\sim$1.7 μ_B) moments.

Acknowledgments

This research was partially supported by the Ministry of Education, Culture, Sports, Science and Technology, Japan, a Grant-in-Aid for Young Scientists (No. 16750043) and Scientific Research Priority Area 'Panoscopic assembling and high ordered functions for rare earth materials' (No 17042003).

References

[1] Maeno Y, Hashimoto H, Yoshida K, Nishizaki S, Fujita T, Bednorz J G and Lichtenberg F 1994 *Nature* **372** 532–4
[2] Callaghan A, Moeller C W and Ward R 1966 *Inorg. Chem.* **5** 1572–6
[3] Greatrex R, Greenwood N N, Lal M and Fernandez I 1979 *J. Solid State Chem.* **30** 137–48
[4] Gibb T C and Greatrex R 1980 *J. Solid State Chem.* **34** 279–88
[5] Battle P D, Goodenough J B and Price R 1983 *J. Solid State Chem.* **46** 234–44
[6] Battle P D and Macklin W J 1984 *J. Solid State Chem.* **52** 138–45
[7] Battle P D and Macklin W J 1984 *J. Solid State Chem.* **54** 245–50
[8] Battle P D and Jones C W 1989 *J. Solid State Chem.* **78** 108–16
[9] Battle P D, Jones C W and Studer F 1991 *J. Solid State Chem.* **90** 302–12
[10] Doi Y and Hinatsu Y 1999 *J. Phys.: Condens. Matter* **11** 4813–20
[11] Doi Y, Hinatsu Y, Oikawa K, Shimojo Y and Morii Y 2000 *J. Mater. Chem.* **10** 797–800
[12] Doi Y, Hinatsu Y, Oikawa K, Shimojo Y and Morii Y 2000 *J. Mater. Chem.* **10** 1731–7

[13] Izumiyama Y, Doi Y, Wakeshima M, Hinatsu Y, Oikawa K, Shimojo Y and Morii Y 2000 *J. Mater. Chem.* **10** 2364–7
[14] Izumiyama Y, Doi Y, Wakeshima M, Hinatsu Y, Shimojo Y and Morii Y 2001 *J. Phys.: Condens. Matter* **13** 1303–13
[15] Izumiyama Y, Doi Y, Wakeshima M, Hinatsu Y, Nakamura A and Ishii Y 2002 *J. Solid State Chem.* **169** 125–30
[16] Doi Y, Hinatsu Y, Nakamura A, Ishii Y and Morii Y 2003 *J. Mater. Chem.* **13** 1758–63
[17] Hinatsu Y, Izumiyama Y, Doi Y, Alemi A, Wakeshima M, Nakamura A and Morii Y 2004 *J. Solid State Chem.* **177** 38–44
[18] Parkinson N G, Hatton P D, Howard J A K, Ritter C, Ibberson R M and Wu M M 2004 *J. Phys.: Condens. Matter* **16** 7611–24
[19] Sakai C, Doi Y and Hinatsu Y 2005 *J. Alloys Compounds* at press doi:10.1016/j.jallcom.2005.01.090
[20] Ohoyama K, Kanouchi T, Nemoto K, Ohashi M, Kajitani T and Yamaguchi Y 1998 *Japan. J. Appl. Phys.* **37** 3319–26
[21] Rodrigues-Carvajal J 1993 *Physica* B **192** 55–69
[22] Parkinson N G, Hatton P D, Howard J A K, Ritter C, Chien F Z and Wu M K 2003 *J. Mater. Chem.* **13** 1468–74
[23] Izumiyama Y and Hinatsu Y, unpublished results
[24] Gordon J E, Fisher R A, Jia Y X, Phillips N E, Reklis S F, Wright D A and Zettl A 1999 *Phys. Rev.* B **59** 127
[25] Van Vleck J H 1932 *The Theory of Electric and Magnetic Susceptibilities* (Oxford: Clarendon)
[26] Bonrath H, Hellwege K H, Nicolay K and Weber G 1966 *Phys. Kondens. Mater.* **4** 382–90